

The properties of salt-filled sodalites Part 2. Synthesis, decomposition reactions and phase transitions of nitrate sodalite $\text{Na}_8[\text{AlSiO}_4]_6(\text{NO}_3)_2$

J.-Ch. Buhl

Institut für Mineralogie, Universität Münster, Corrensstr. 24, W-4400 Münster (Germany)

(Received 28 January 1991)

Abstract

Nitrate sodalites, $\text{Na}_8[\text{AlSiO}_4]_6(\text{NO}_3)_2$, have been synthesized hydrothermally (570 K, 0.1 GPa) using zeolite A, sodium nitrate and 8 M NaOH. IR spectroscopy indicates clearly the enclathration of NO_3^- exclusively within the sodalite cages (absorption band at 1380 cm^{-1}). ^{29}Si -MAS-NMR confirms the alternating ordering of silicon and aluminium in the nitrate sodalite framework, according to a single peak at $\delta = -86.7$ ppm for Si(4Al) units.

From the DTA and calorimetric investigations a reversible structural phase transition has been identified for $\text{Na}_8[\text{AlSiO}_4]_6(\text{NO}_3)_2$, starting at temperatures between 920 K (DTA) and 930 K (DSC). High temperature Guinier–Simon photographs reveal the onset of a maximal framework expansion of the nitrate sodalite at temperatures $T_{\text{tr}} \geq 920$ K. The observed thermal decomposition behaviour and the corresponding evaluation of the unit-cell volume indicate special host–guest interactions due to the dynamics of the enclosed NO_3^- .

INTRODUCTION

Sodalites, consisting of sodalite cages as basic structural building blocks, offer an attractive model system for the zeolites A, X and Y. In addition to cation exchange and substitution of framework T-atoms, the enclathration of several guest species yields new information on the reactivity and thermal stability of porous tectosilicates [1–4].

Recent investigations on the hydrothermal synthesis of sodium-nitrite-incorporated sodalites gave evidence for a partial transformation of NO_2^- to NO_3^- within the polyhedral cages during synthesis [5,6], as well as during heating of nitrite sodalite in air [7–9]. Therefore this study investigates the method of direct synthesis of nitrate-occluded sodalites and the properties of this new phase.

EXPERIMENTAL

Nitrate sodalites, $\text{Na}_8[\text{AlSiO}_4]_6(\text{NO}_3)_2$, were synthesized hydrothermally at 570 K and 0.1 GPa pressure in steel autoclaves of 18 ml capacity. 50 mg

of Zeolite A (Fluka 69836) were mixed with 320 mg sodium nitrate (Merck 6537) and 1 ml of 8 M NaOH solution (Merck 6495) and sealed into silver liners, 80 mm in length and 8 mm in diameter. After a reaction period of 24 h the crystalline products were washed with water and dried at 350 K for 1 h. The crystals were examined by X-ray powder diffraction (Guinier method) as well as by IR spectroscopy (Perkin-Elmer spectrometer 683) and ^{29}Si - and ^{23}Na -MAS-NMR (Bruker MSL-400 MAS-NMR spectrometer). The thermal properties of the new sodalite were followed by simultaneous thermal analysis, including TG, DTG and DTA (Mettler thermoanalyser TA 146) and by high temperature X-ray powder diffractometry in the temperature interval between 293 and 1120 K using the Enraf-Nonius high temperature Guinier-Simon camera (heating rate 16 K h^{-1}). Calorimetric measurements on a Perkin-Elmer differential scanning calorimeter DSC-7 and high temperature X-ray powder diffractometry were used to study the phase transition behaviour of the nitrate sodalite.

RESULTS

Synthesis and characterization

Single crystals of average dimension 0.35 mm were obtained, with the well-known cubo-octahedral habit of sodalites. A microphotograph of a typical hydrothermal product is shown in Fig. 1. The formula

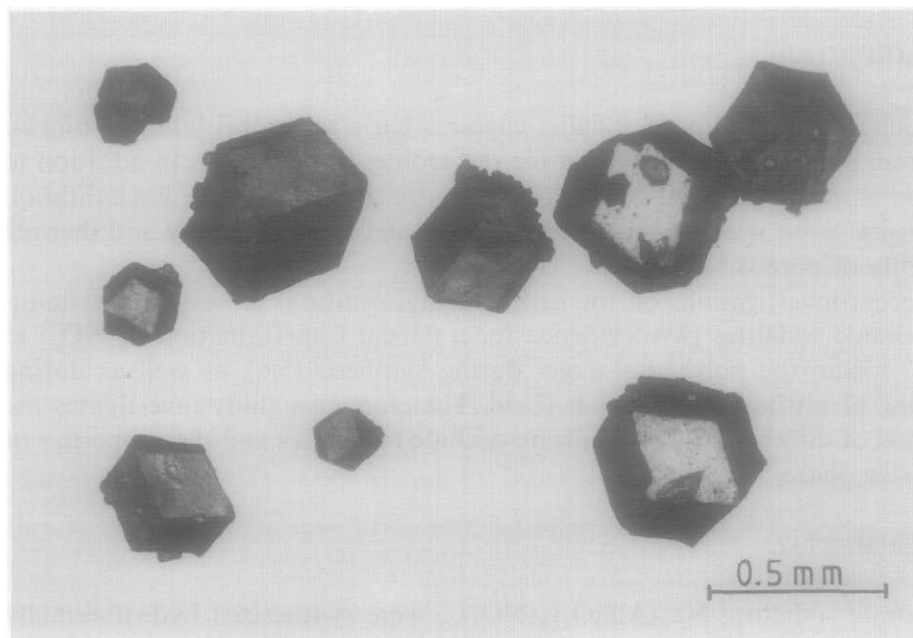


Fig. 1. Microphotograph of nitrate sodalite single crystals.

TABLE 1

X-ray powder data of nitrate sodalite at 298 K: $\text{Na}_8[\text{AlSiO}_4]_6(\text{NO}_3)_2$, cubic, $a_0 = 8.9876(1)$ Å

hkl	$2\theta_{\text{obs}}$	d_{obs}	I/I_0
1 1 0	13.934	6.351	71
2 0 0	19.769	4.487	29
2 1 1	24.278	3.663	100
3 1 0	31.490	2.839	67
2 2 2	34.584	2.592	100
3 2 1	37.453	2.399	45
4 0 0	40.141	2.245	25
3 3 0	42.693	2.116	95
4 1 1			
3 3 2	47.458	1.914	12
4 2 2	49.708	1.833	26
4 3 1	51.888	1.761	59
5 1 0			
4 4 0	58.072	1.587	45
4 3 3	60.039	1.540	50
5 3 0			
4 4 2	61.964	1.496	41
6 0 0			
5 3 2	63.860	1.457	46
6 1 1			
6 2 0	65.726	1.420	8
5 4 1	67.559	1.385	18
6 2 2	69.374	1.354	37
6 3 1	71.165	1.324	30
4 4 4	72.937	1.296	24
5 4 3	74.690	1.270	16
5 5 0			
7 1 0			
5 5 2	78.164	1.222	44
6 3 3			
7 2 1			
6 4 2	79.882	1.200	14
7 3 0	81.593	1.179	12
6 5 1	84.998	1.140	15

$\text{Na}_8[\text{AlSiO}_4]_6(\text{NO}_3)_2$ was confirmed as the composition for the sodalites obtained using the different analytical methods described above (X-ray powder diffractometry, IR spectroscopy and ^{29}Si -MAS-NMR, as well as thermogravimetry). X-ray powder diffraction studies yielded the well-known sodalite pattern [1–4]; the powder diffraction data of nitrate sodalite are summarized in Table 1. The observed unit cell parameter, $a_0 = 8.9876(1)$ Å, also indicates nitrate incorporation within the sodalite cages, when com-

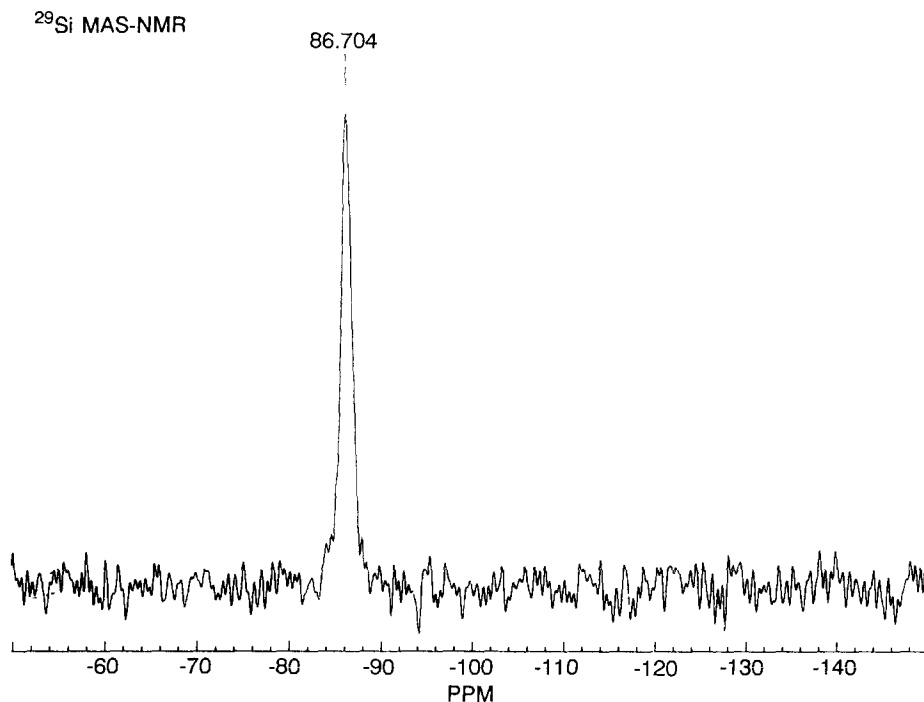


Fig. 2. ^{29}Si -MAS-NMR spectrum of nitrate sodalite.

pared with the values for species with 100% cage-filling with molecules like NaOH or NaNO_2 [1,4].

The Si/Al ratio of nitrate sodalite can be observed from ^{29}Si -MAS-NMR spectroscopy. The ^{29}Si -MAS-NMR spectrum of $\text{Na}_8[\text{AlSiO}_4]_6(\text{NO}_3)_2$ was recorded at 79.5 MHz with a multinuclear double-bearing probe. It shows a sharp symmetrical peak of Si(4Al) units with a chemical shift of $\delta = -86.7$ ppm, as can be seen from Fig. 2. This confirms the alternating ordering of Si and Al atoms in the framework and the Si/Al ratio of 1.0 [10]. The ^{23}Na -MAS-NMR spectrum of nitrate sodalite exhibits a typical quadrupole pattern, suggesting a dynamic averaging of an orientational disorder of the NO_3^- anions in the sodalite cages. The coordination of the sodium atoms should be characterized by a non-spherically symmetric charge distribution with slight deviations from axial symmetry. A more detailed study of structural features by combined methods of X-ray single-crystal diffraction and ^{23}Na -MAS-NMR spectroscopy is in preparation.

The IR spectrum of NO_3^- -sodalite is shown in Fig. 3. In addition to the symmetric and asymmetric T-O-T stretching and the symmetric O-T-O bending modes, which are typical of aluminosilicate sodalites [11], the nitrate absorption band at 1380 cm^{-1} could be observed. No water molecules or hydroxide, not carbonate from CO_2 impurities in the starting materials of the hydrothermal synthesis, seemed to be incorporated during

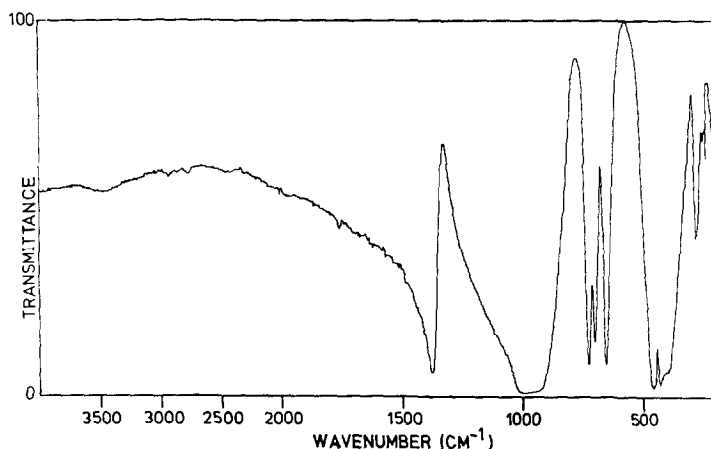


Fig. 3. IR spectrum of nitrate sodalite.

crystal growth. The results of simultaneous thermal analysis of nitrate sodalite, including thermogravimetry (TG), differential thermogravimetry (DTG) and differential thermoanalysis (DTA), are given in Fig. 4. The measurements indicate a reversible phase transition, suggested by an endothermic DTA signal with an onset temperature of 920 K, without any weight loss. The reversible character of this phase transition is demonstrated in Fig. 5. Here, two cycles of heating and cooling of a nitrate sodalite sample on the thermobalance show clearly the nature of the endothermic and exothermic peaks of the transitions. More features of this structural transition are given below.

As can be seen from Fig. 4, the decomposition of the enclathrated nitrate occurs in a two-step reaction with endothermic DTA maxima of 1330 and

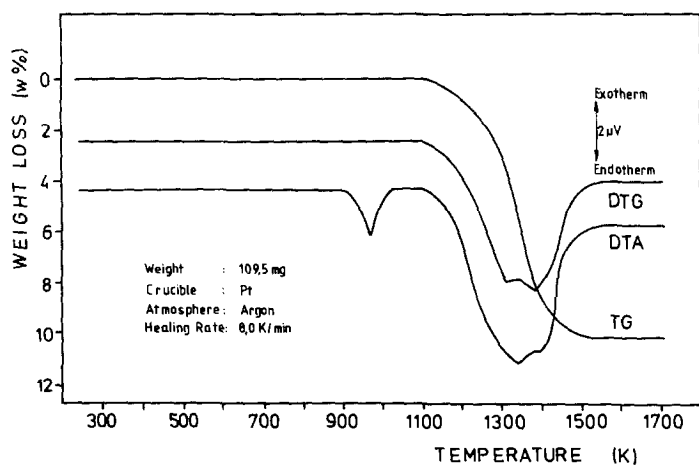


Fig. 4. Simultaneous thermal analysis of nitrate sodalite.

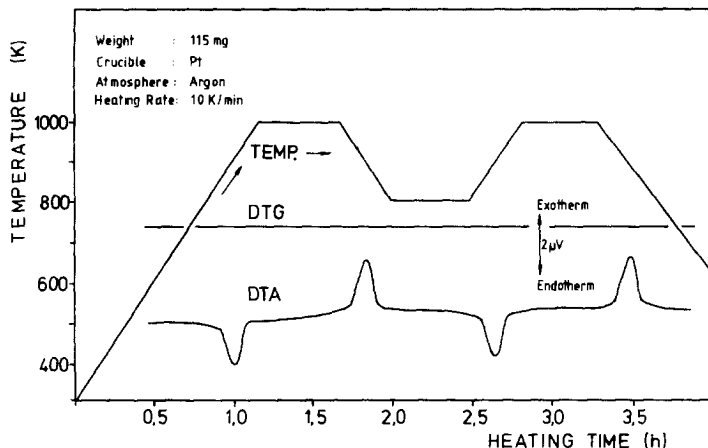


Fig. 5. Reversible phase transition according to DTA/TG measurements during two cycles of heating and cooling.

1400 K. The second step marks the total destruction of the sodalite framework at elevated temperatures. Additional X-ray powder diffraction data (Guinier technique) indicate the formation of a nepheline-like phase after the total collapse of the sodalite framework. The plot of the course of the unit cell volume during heating of the nitrate sodalite (TG curve), as calculated from a Guinier–Simon photograph, is shown in Fig. 6 (heating rates 0.3 K min^{-1} for the X-ray heating experiment and 8 K min^{-1} for the thermogravimetry). An increase in the cell volume during heating can be observed from this figure, up to the temperature of the onset of the phase transition. Here the framework expansion reaches its maximum ($V_{295 \text{ K}} = 727$

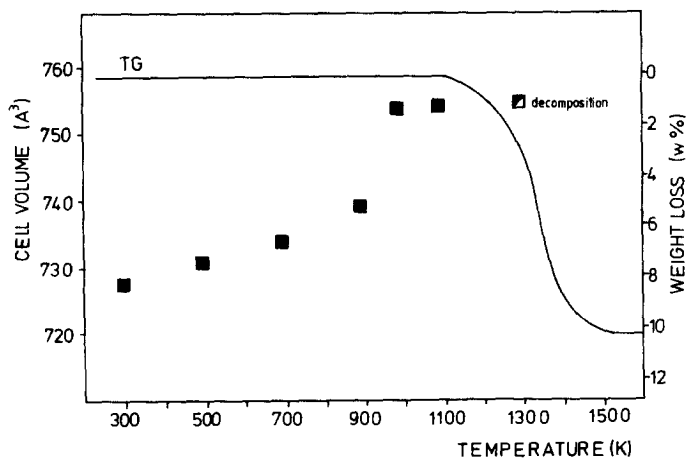


Fig. 6. The change in the unit-cell volume during thermal decomposition of nitrate sodalite (heating rate 0.3 K min^{-1} for the X-ray diffraction experiment and 8 K min^{-1} for the thermogravimetry).

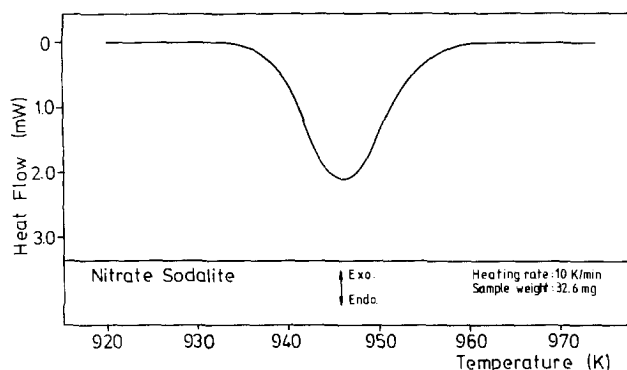


Fig. 7. The course of the heat flow (DSC) with temperature during the structural phase transition of nitrate sodalite.

\AA^3 , $V_{920\text{K}} = 769 \text{\AA}^3$). In the following temperature interval up to the destruction of the sodalite structure, the framework volume is nearly constant (apart from a very small increase due to normal thermal expansion).

The reversible phase transition of nitrate sodalite was investigated further on the basis of differential scanning calorimetric measurements, as well as by high temperature X-ray powder diffractometry. The course of the heat

TABLE 2

X-ray powder data of nitrate sodalite at 970 K obtained from a Guinier–Simon film: $\text{Na}_8[\text{AlSiO}_4]_6(\text{NO}_3)_2$, cubic, $a_0 = 9.162(1) \text{\AA}$

hkl	$2\theta_{\text{obs}}$	d_{obs}	I/I_0
1 1 0	13.737	6.441	37
2 0 0	19.601	4.525	9
2 1 1	23.934	3.715	100
3 1 0	31.049	2.878	19
2 2 2	34.105	2.627	40
3 2 1	36.989	2.428	15
4 0 0	39.592	2.275	14
3 3 0	42.103	2.144	26
4 1 1			
3 3 2	46.866	2.429	5
4 3 1	51.151	1.784	19
5 1 0			
4 4 0	57.172	1.610	9
4 3 3	59.108	1.562	11
5 3 0			
4 4 2	60.876	1.521	9
6 0 0			
5 3 2	62.884	1.477	11
6 1 1			

flow with temperature during the structural phase transition, according to a typical DSC curve for nitrate sodalite, is given in Fig. 7.

The X-ray powder data obtained from a Guinier–Simon photograph (taken up to a diffraction angle of $2\theta = 64^\circ$) for the high temperature phase of nitrate sodalite are given in Table 2. A lattice parameter of $a_0 = 9.162(1)$ Å can be estimated for the temperature of 970 K. The absence of the (4 2 2) reflection for the high temperature form, as well as remarkable deviations in the relative intensities of the two phases, can be noted by comparing Tables 1 and 2. The observed high temperature phase transition of nitrate sodalite from a phase of cubic symmetry to another cubic phase, seems to be the result of specific host–guest interactions that are a result of the dynamics of the enclosed NO_3^- and Na^+ ions. In addition to the positional disorder of the nitrate within the sodalite cages, the initiation of some movement of the sodium cations inside the sodalite matrix should also be taken into account. Further structural studies above and below the transition temperature are currently in progress, in order to provide definitive evidence concerning the position and disorder of the cage-filling ions and their dynamic characters.

ACKNOWLEDGEMENTS

The author thanks Mrs. A. Breit for excellent technical assistance, Dr. G. Engelhardt (University of Stuttgart) for the MAS–NMR results, Professor J. Grobe (Münster) for permission to use the IR spectrometer in his laboratory, and G. Wildermuth (University of Konstanz) for the DSC measurements.

REFERENCES

- 1 J. Felsche and S. Luger, *Thermochim. Acta*, 113 (1987) 35.
- 2 J.-Ch. Buhl, G. Engelhardt and J. Felsche, *Zeolites*, 9 (1989) 40.
- 3 J.-Ch. Buhl, *Thermochim. Acta*, 168 (1990) 253.
- 4 F. Hund, *Z. Anorg. Allg. Chem.*, 511 (1984) 255.
- 5 J.-Ch. Buhl, Ch. Gurriss and W. Hoffmann, in J.C. Jansen, L. Moscou and M.F.M. Post (Eds.), *Proc. 8th Int. Zeol. Conf., Zeolites For The Nineties*, Amsterdam, 1989, p. 23.
- 6 J.-Ch. Buhl, *J. Solid State Chem.*, 91 (1991) 16.
- 7 J.-Ch. Buhl, J. Löns and W. Hoffmann, *Ber. Dtsch. Miner. Ges.*, 1 (1989) 20.
- 8 J.-Ch. Buhl, Ch. Gurriss and W. Hoffmann, *Ber. Dtsch. Miner. Ges.*, 1 (1989) 19.
- 9 M.T. Weller, G. Wong, C.L. Adamson, S.M. Donald and J.J.B. Roe, *J. Chem. Soc., Dalton Trans.*, (1990) 53.
- 10 G. Engelhardt, S. Luger, J.-Ch. Buhl and J. Felsche, *Zeolites*, 9 (1989) 182.
- 11 E.M. Flanigen and H. Khatami, *Advances in Chemistry Series*, 16 (1971) 201.